In-Depth Study of the Electronic Properties of NIR-Emissive κ3N Terpyridine Rhenium(I) Dicarbonyl Complexes

n-Depth Study of the Electronic Properties of NIR-Emissiveκ3NTerpyridine Rhenium(I) Dicarbonyl Complexes

Thomas Auvray, Benedetta Del Secco, Amélie Dubreuil, Nelsi Zaccheroni,* and Garry S. Hanan*

Inorg. Chem. 2021, 60, 1, 70–79

In-depth study of the electronic properties of NIR emissive κ^3N terpyridine rhenium(I) dicarbonyl complexes

Thomas Auvray,[a] Benedetta Del Secco,[b] Amélie Dubreuil,[a] Nelsi Zaccheroni,[b*] and Garry S. Hanan[a]*

[a] Département de Chimie, Université de Montréal, Montréal, Canada, H2V-0B3

[b] Dipartimento di Chimica 'G. Ciamician',Università degli Studi di Bologna, Via S.Giacomo 11, 40126, Bologna, Italy

Abstract

The structure-properties relationship in a series of carbonyl rhenium(I) complexes based on substituted terpyridine ligands of general formula $[Re(\kappa^x N\text{-}Rtpy)(CO)_yL]^{n+}$ is explored by both experimental and theoretical methods. In these compounds, the terpyridine ligands adopt both bidentate (κ^2N) and terdentate (κ^3N) coordination modes associated with three or two carbonyls, respectively. Conversion from the κ^2N to the κ^3N coordination mode leads to large changes in the absorption spectra and oxidation potentials due to destabilization of the HOMO level of each complex. The κ^3N complexes' absorption profiles cover the whole visible spectra with lower maxima around 700 nm, tailing out to 800 nm, while no emission is observed with Br^- as axial ligand L. When the axial ligand is modified from the native halide to pyridine or triphenylphosphine, the lowest absorption band is blueshifted by 60 and 90 nm, respectively. These cationic complexes are near-infrared emitters with emission maxima between 840-950 nm for the pyridine compounds and 780-800 nm for the triphenylphosphine ones.

Introduction

The chemistry of rhenium(I) complexes has sparked a tremendous amount of research efforts over the past decades. Their photophysical and electrochemical properties have been thoroughly studied[1-5] and applied in a multitude of fields such as solar energy harvesting devices[6] and solar-to-chemical energy conversion,[7-11] light emitting devices[12, 13] as well as photodynamic therapy and cellular imaging.[14, 15] While the breadth of their application is large, most of the studies regarding these complexes follow the seminal work from J.M. Lehn,[10] T.J. Meyer[11] and coworkers who showed in the 1980's that

[$Re(CO)_3(bpy)X$] complexes (where bpy is 2,2'-bipyridine and X is a halide) are able to catalyze the selective reduction of carbon dioxide into carbon monoxide either photo- or electrochemically. Their photophysical properties were also applied to photocatalytic hydrogen evolution, using the Re(I) complex as photosensitizer with a cobalt catalyst.[9, 16] Efforts focused on tuning the photophysical properties of the complexes lead to several structural variations, either by modification of the diimine core[17-20] or by introduction of other ligands such as phosphine,[21-27] N-heterocyclic carbene,[28] alcyne[29, 30] or isocyanide.[31, 32] These complexes were also used as building blocks in supramolecular assemblies[33-36] and extended periodic structures.[37, 38]

We recently focused on tridentate ligand-based complexes as they offer a suitable geometry for predictable assembly depending on the facial or meridional arrangement of the ligands. Others investigated related complexes at the same time, leading to the report of several complexes with tridentate N,N,N ligand in a meridional[39-42] or facial geometry[43, 44] (Fig. 1). Interestingly, the meridionally coordinated κ^3N terpyridine and N,N,N pincer based complexes[45] proved to have extended absorption in the visible compared to their κ^2N equivalent, or the facial isomers, which usually exhibit absorption limited to the high energy visible, with some exception involving excited state mixing with other absorbing units.[46] In a recent report, Dempsey and coworkers, working with a Re bipyridine complex, successfully pushed its absorption to the low energy visible region, matching the κ^3N terpyridine values, by modifying the nature of the ligands completing the coordination sphere.[47]

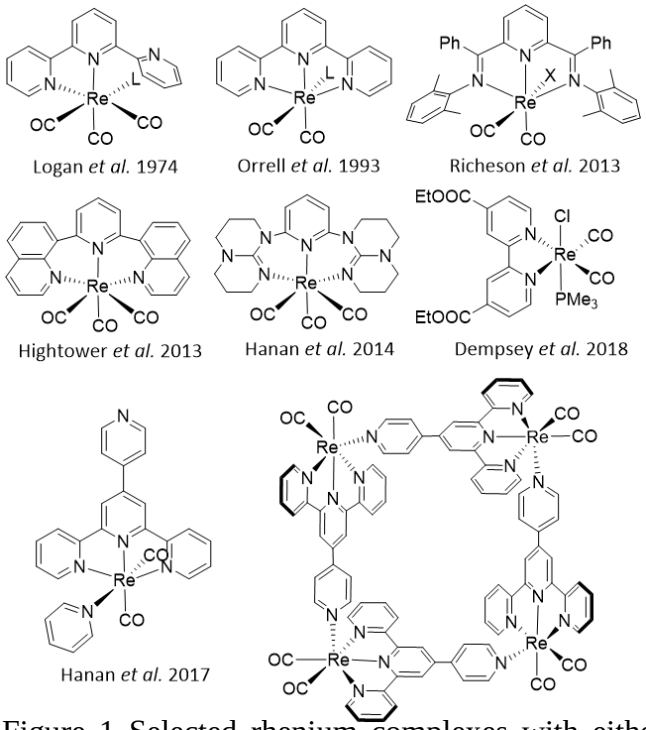

Figure 1 Selected rhenium complexes with either similar N,N,N coordination or related properties.

However, to our knowledge, our report of the κ^3N terpyridine based complex $[Re(CO)_2(py)(\kappa^3N\text{-}4pytpy)]^+$ and the corresponding metallasquare (with *py* standing for pyridine and *4pytpy* for 4'(4-pyridyl)-2,2':6',2''-terpyridine) is the only case where this type of complex was shown to possess a near-infrared emission band at room temperature, with an emission maximum around 950 nm.[36] The study of the κ^2N and κ^3N terpyridine complexes has been the object of successive corrections in the literature following technological improvements of spectrophotometers. As an example, in their initial report, Lehn and coworkers observed only emission in cryogenic condition for the κ^2N complex, which are now found to be applicable in luminescent devices.[12, 17] We thus decided to investigate the effect of varying substituent and ancillary ligand on the emission of κ^3N terpyridine rhenium complexes in order to gain a better understanding of the parameters influencing their electronic properties.

Results and discussion

Synthesis

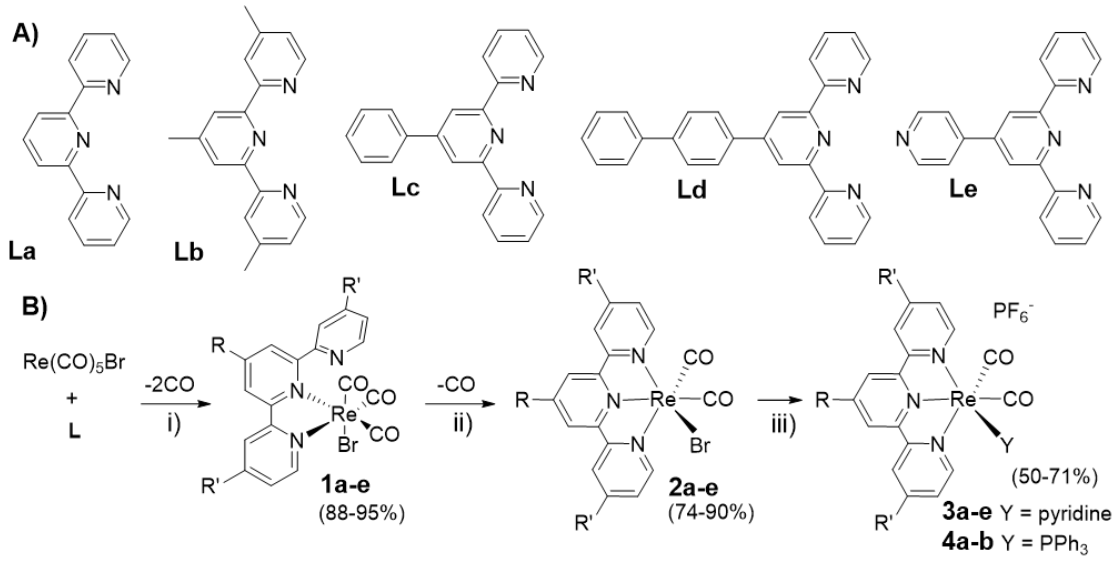

Figure 2 A) Selected substituted terpyridines; B) Synthetic pathways for the complexes. i) toluene, reflux, 4 h; ii) under N_2, 270 °C, 6 h; iii) for **3a-e**: pyridine, AgOTf (1.25 eq.), reflux 5 h, $KPF_{6(aq)}$, for **4a-b**: THF, PPh_3, AgOTf (1.25 eq.), reflux 5 h, $KPF_{6(aq)}$

We chose the terpyridine ligands presented in Fig. 2A to study the effect of the substituent on the photophysical properties of the targeted complexes. The detailed synthesis for each compound can be found in the supporting information. The κ^2N tpy coordinated complexes **1a-e** were prepared following classical Re tricarbonyl diimine preparation procedures from $Re(CO)_5Br$ (Fig. 2B) in excellent yield (88-95%). The loss of a third CO is known to require harsher conditions such as UV irradiation,[48] oxido-decarbonylation[47, 49] or pyrolysis.[39] The tricarbonyl complexes obtained were converted into the dicarbonyl κ^3N form **2a-e** using the latter. The targeted quantity of the suitable complex **1a-e** was placed in an oven dried vial which was then sealed in a glovebox to maintain an inert atmosphere throughout the reaction. This vial was then placed in a sand bath heated to 270°C. The solids changed color as the reaction proceeded, from orange/yellow to dark brown/black. This procedure yielded the corresponding complexes **2a-e** in good to excellent yield (74-90%), but manipulation of these solids is made difficult by static electricity. Also, these solids are hygroscopic as shown by NMR and CHN analysis in which water was still observed even after careful drying. Finally, following the procedures reported by Hightower and coworkers,[40] we prepared complexes **3a-e** and **4a-b** by bromide abstraction with silver triflate, followed by replacement either by pyridine or triphenylphosphine. These cationic complexes were isolated in medium to good yield (50-71%) as their PF_6^- salts and purified on alumina to remove any unreacted materials or silver salt. The lower yield comes from losses in the precipitation step in water. Interestingly, the neutral complexes **1a-e** and **2a-e** have lower solubility in common solvents than the cationic complexes **3a-e** and **4a-b**.

Structural characterization

To confirm the identity and purity of all the complexes, we used a combination of ^{1}H and ^{13}C NMR spectroscopy, infrared (IR) spectroscopy, mass spectrometry (MS) and elemental analysis (CHN). All compounds were observed by MS as mono-cationic species presenting the typical pattern of rhenium compounds caused by its two natural isotopes ^{185}Re and ^{187}Re (with 37/63 % abundancy). The NMR spectra of complexes **1a-e** (Fig. S1-S5) confirm the lower symmetry expected for the κ^2N coordination of the ligand, which leads to no equivalent center except for the ortho and meta positions of the 4'aryl substituent in **Lc-e**. In some cases, we observed splitting of signals that we ascribed to the

fluxionality of such complexes. Indeed, the rhenium center can move between the two bidentate coordination sites *via* different mechanisms well documented by Orrell *et al.* and others using variable temperature NMR studies.[39, 50-53] The facial geometry was confirmed by solid state IR spectroscopy where the characteristic bands for the CO vibrations were observed, the experimental and theoretical values obtained by DFT being listed in Table S1. No clear effect of the donor / acceptor substituent can be seen for these data, with similar values for all compounds of the same family. The κ^3N coordinated complexes **2a-e** obtained by pyrolysis present symmetrical NMR spectra, typical for meridional terpyridine based complexes (Fig. S6-S10). The *mer*-tpy, *cis*-CO conformation was confirmed by IR spectroscopy with the expected two bands for the CO vibrations. These bands are shifted to lower wavenumber compared to the κ^2N complexes **1a-e**, from an average of 2020, 1910 and 1880 cm^{-1} to 1880 and 1800 cm^{-1}, respectively (Table S1). This shift is due to the back-donation from the d^6 metal center being now only shared between the two remaining carbonyl ligands. This shift is also indicative of a somewhat more electron rich metal center, which would be easier to oxidize. The NMR spectra of **3a-e** (Fig. S11-S15) and **4a-b** (Fig. S16-S17) are like those of **2a-e**, with additional peaks from the pyridine or phosphine ligand, respectively. Replacing the bromide by a pyridine has moderate effect on the CO vibrations bands that are shifted to slightly higher wavenumbers ($\Delta\nu \approx 20$ cm^{-1}), a more significant shift being observed in the case of **4a-b** with a triphenylphosphine ligand ($\Delta\nu \approx 40$ cm^{-1}) (Table S1). These variations were predicted by DFT calculations (*vide infra*) and indicate a trend in ease of oxidation, i.e. **2a-e** should be easier to oxidize than **3a-e**, followed by **4a-b** and finally **1a-e**. A similar trend was presented recently by Dempsey and coworkers on a series of Re-bipyridine compounds.[47]

Computational studies

In parallel to the synthesis of the targeted compounds, we performed DFT calculations to model them, using Gaussian16 rev. A03, and support our interpretation of the spectroscopic measurements. We used the hybrid PBE0 method with the LanL2DZ basis set for all atoms. All calculations were performed without symmetry constraints and the effect of the solvent (acetonitrile) was included via a conductor-like polarizable continuum (CPCM). Frequency calculations after optimization were performed to

confirm that local minima had been reached and obtain theoretical vibrational values (see Table S1). The energy diagram presented in Fig. 3 allows for a simple observation of the trend predicted for the successive modifications leading to complexes **1**, **2**, **3** or **4**. The energy values for orbitals from LUMO+2 to HOMO-2 with their Mulliken population analysis are reported in Tables S2-S18.

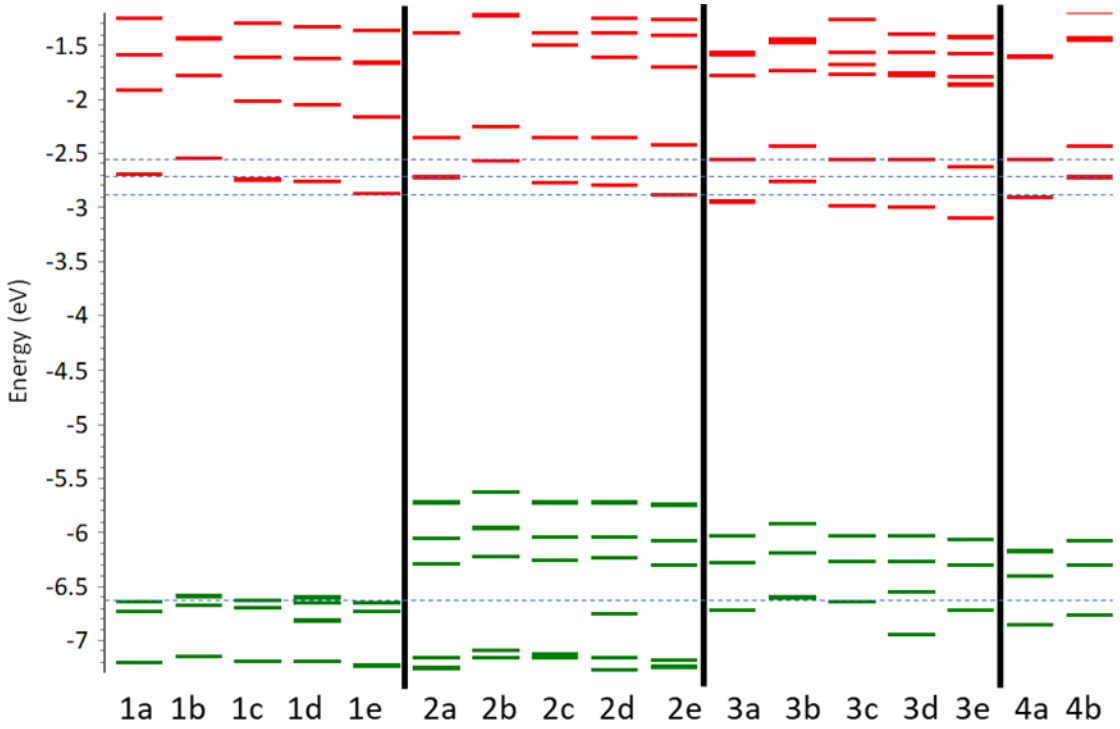

Figure 3 Partial energy diagram centered on frontier orbitals for all complexes modeled in an acetonitrile continuum by DFT (PBE0/LanL2DZ).

The conversion of **1a-e** into **2a-e**, i.e. from κ^2N to κ^3N coordination mode, causes a significant increase in energy for the higher occupied levels, i.e. by almost 1eV. This change is expected as the replacement of a strongly π-accepting CO ligand by the weak π-accepting pyridine of the terpyridine ligand should lead to destabilization of the metal centered π orbitals. In addition to the contribution from the bonding π-backdonation between rhenium and carbonyls in **1a-e**, the HOMO and HOMO-1 levels also have an antibonding π* character linked to the donation from the bromide (Fig. 4). This antibonding interaction has a lower contribution in the κ^3N complexes **2a-e**. This can be explained by the destabilization of the metal centered π orbital which reduces the mixing

between the bonding π overlap corresponding to the retrodonation to the carbonyl and the antibonding π overlap associated with the donation from the bromide.

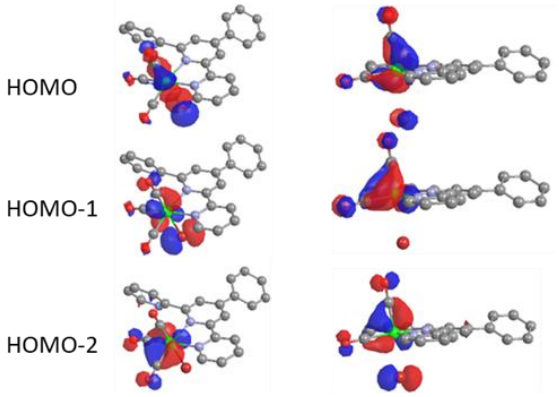

Figure 4 Selected molecular orbitals (isovalue 0.05 e/Å^3) for complexes **-1c** and **-2c** (top to bottom: HOMO to HOMO-3)

Considering the LUMO of **1a-e** and **2a-e**, almost no energy variation is observed, while the LUMO+1 are stabilized by 250 to 480 meV and the LUMO+2 destabilized to a lesser extent. These changes result from the increased conjugation of the terpyridine once in its meridional coordination mode. The LUMO of complexes **1a-e** is delocalized over the coordinated bipyridine-like moiety and the increase in conjugation does not really affect its energy while the LUMO+1 and LUMO+2 involve individual pyridine rings and the extended conjugation modifies their related energies. Going from the neutral **2a-e** to the cationic complexes **3a-e** and **4a-b** leads to an overall stabilization by several hundred meV, with a stronger impact on the occupied levels from the σ-donating triphenylphosphine in **4a-b** compared to the pyridine in **3a-e**.

The different substituents introduced on the terpyridine ligand appear, however, to have a minor effect on the energy level as observed in Fig. 3. The largest effect comes from trimethyl substituted ligand **Lb**, a stronger donor, resulting in a general destabilization of all orbitals for the corresponding complexes. In the case of the phenyl (**Lc**) or biphenyl (**Ld**) substituent on the 4' position, they caused only a slight stabilization of the LUMO compared to the parent compound. Interestingly, however, **Ld** based complexes exhibit significant contribution of the biphenyl in the HOMO-2 level of all complex and the HOMO in **1d**. The 4-pyridyl in **Le** leads to a lower LUMO in its related complexes, as expected from an electron accepting substituent. **Lc**, **Ld** and **Le** exhibit contributions of the aromatic ring in the 4' position to the LUMO+2, reducing the impact of the κ^2N to κ^3N conversion on its energy compared to the LUMO+1 as mentioned above.

Furthermore, as we were expecting large differences in the photophysical properties between κ^2N and κ^3N complexes, based on previous reports,[36, 44] we conducted time dependent DFT (TD-DFT) calculations to provide information regarding the positions and nature of the electronic transitions. The natural transition orbitals[54] for the lowest allowed singlet-to-singlet transition and the lowest forbidden singlet-to-triplet transition of each complex are reported in Figure S18-S34 while the calculated transitions are represented in Fig. S35-S51 along with the experimental spectra (*vide infra*). In all cases, the lowest energy transitions are mainly corresponding to the HOMO-LUMO transition and can be describe as a combination of a metal-to-ligand charge transfer (MLCT, i.e. Re(d)→L(π*)) with various ligand-to-ligand charge transfer (LLCT) transitions involving either the Br^- or the CO. In the triplet transitions of the κ^2N complexes **1a-e**, especially in **1c**, the model indicates contribution of a ligand centred transition (LC, i.e. π→π*). In these κ^2N compounds, there is also a non-negligible contribution of the Br^-(n)→L(π*) LLCT transition, leading a complex mix of transitions, as modeled by others in the literature[4, 55] and experimental proved using X-ray absorption spectroscopy.[56] The contribution of the LC and LLCT transitions are reduced after conversion to the κ^3N coordination, following the change in orbital contributions discussed above. There is, however, an increased contribution from the orbital corresponding to the backdonation from the Re(I) to the carbonyls, the transitions are thus better described as a metal-ligand-to-ligand charge transfers (MLLCT, {$Re(CO)_2$}→L(π*)). Following the removal of the Br^- in **3a-e** and **4a-b**, the MLLCT becomes the only contributing transition, according to the theoretical model.

The TD-DFT predicted emission values give unreasonable values for rhenium or iridium complexes and more precise values can be obtained by calculating the energy of the optimized geometry of the first triplet, as well as the energy of the singlet state in the same geometry, as described by Zysman-Colman[57] and coworkers, giving the values in Table 1.

Table 1 Calculated wavelengths for the $S_0 \rightarrow T_1$ transition corresponding to the expected emission wavelengths.

Complex	**1a**	**1b**	**1c**	**1d**	**1e**	**2a**	**2b**	**2c**	**2d**
$\lambda_{TD\text{-}DFT}$ / nm	444.0	434.0	457.6	479.2	460.6	691.1	663.8	696.4	698.0
$\lambda_{0,0}$ / nm	476.5	466.0	493.7	502.0	510.1	808.0	778.8	819.5	822.7
λ_{ae} / nm	580.8	553.3	615.6	617.9	649.2	959.1	931.7	972.1	976.0
Complex	**2e**	**3a**	**3b**	**3c**	**3d**	**3e**	**4a**	**4b**	
$\lambda_{TD\text{-}DFT}$ / nm	722.6	670.2	639.3	671.4	672.6	693.9	610.1	582.4	
$\lambda_{0,0}$ / nm	865.9	779.8	754.2	786.4	788.3	826.4	699.1	684.9	
λ_{ae} / nm	1042.0	924.3	900.1	929.5	932.6	989.9	854.8	822.3	

$\lambda_{TD\text{-}DFT}$ = wavelength of $S_0 \rightarrow T_1$ transition obtained by TDDFT at the S_0 optimized geometry

$\lambda_{0,0}$ = 1240/[$E(T_1) - E(S_0)$] at their respective optimized geometries obtained by DFT

λ_{ae} = 1240/[$E(T_1) - E(S_0)$] at the T_1 optimized geometry (adiabatic electronic emission) obtained by DFT

DFT/TD-DFT modelization allowed us to extract trends throughout the family of complexes reported herein. Based on these theoretical values, we expected the reduction potentials of the complexes to show little to no variations while the oxidation potentials should better reflect the variation between the four series. The destabilization of the highest occupied levels would also result in reduced band gaps, which would manifest by a decrease in energy for the lowest absorption band of these compounds. We thus acquired the experimental values using absorption spectroscopy and electrochemistry to confirm the predicted effect of the different structural change.

UV-Vis absorption spectroscopy

The absorption spectrum of each complex was measured in acetonitrile. The absorption maxima and molar absorption coefficient are reported in Table S19, while selected values for the transitions discussed below are displayed in Table 2. The spectra are presented in the supporting material (Fig. S35-S51) with the corresponding calculated transitions from time dependent DFT.

A large bathochromic shift between the κ^2N and κ^3N coordination modes can be observed in Fig. 5 presenting the spectra of the complexes based on **Lb**. While the κ^2N compounds barely absorb in the visible with maxima around 360-390 nm with tailing into the visible region, all the κ^3N complexes absorption spectra cover the whole visible region with

three large additional transitions between 400 nm and 700 nm. The replacement of the bromide by pyridine in **3a-e** leads to a ≈40 nm blueshift, while the triphenylphosphine complexes **4a-b** present an even stronger blueshift of ≈ 80 nm. The transitions in the visible correspond in all cases to Metal-Ligand-to-Ligand Charge Transfer (MLLCT), with the electron originating from an energy level involving the bonding π orbital of the retrodonation from the rhenium center to the carbonyls ligands and being promoted to terpyridine centered energy levels. As discussed earlier, the bonding π orbital is primarily affected by the change of coordination mode and its subsequent effect on the mixing between the different ligand-metal interactions, explaining the large shift in wavelength without major change in localization.

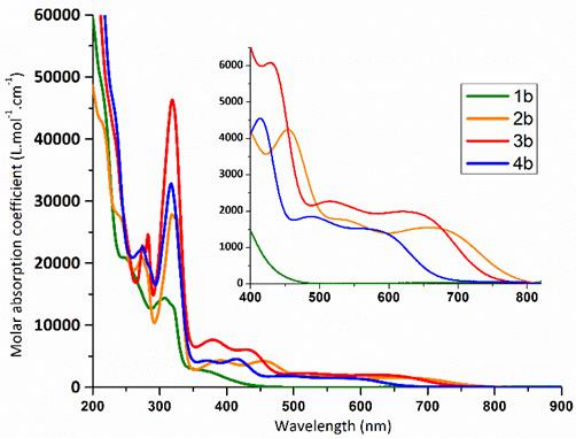

Figure 5 Absorption spectra for all complexes based on ligand **Lb** (measured in acetonitrile)

The various substituents allow for subtle tuning of the absorption maxima, the more electron rich ligand **Lb** leading to shorter wavelengths in all cases, for example. The extended conjugation following introduction of aromatic substituents on the 4' position in the case of **Lc**, **Ld** and **Le** causes a slight redshift compared to **La**. This shift is stronger in the case of the 4-pyridyl substituted ligand **Le**, in agreement with its higher electron withdrawing properties.

Table 2 Absorption maxima and molar absorption coefficients of all complexes in acetonitrile

Complex	λ_{max} / *nm* (ε x10^{-3} $Lmol^{-1}cm^{-1}$)			
1a	367 (2.2)			
2a	395 (3.3)	465 (3.3)	547 (1.2)	690 (1.1)
3a	380 (6.0)	440 (4.8)	516 (1.7)	647 (1.5)
4a	374 (3.2)	421 (3.8)	488 (1.4)	590 (1.1)
1b	360 (2.8)			
2b	390 (4.3)	454 (4.2)	534 (1.8, sh)	660 (1.6)
3b	379 (7.7)	428 (6.1)	514 (2.2)	621 (2.0)
4b	371 (4.3)	415 (4,5)	487 (1.8)	579 (1.5, sh)
1c	386 (3.7)			
2c	398 (4.6)	473 (6.0)	569 (1.3, sh)	700 (1.2)
3c	382 (6.1)	448 (7.0)	529 (1.4, sh)	661 (1.2)
1d	364 (12.6, sh)			
2d	401 (5.8)	475 (8.8)	569 (1.4, sh)	705 (1.4)
3d	386 (8.5, sh)	449 (10.0)	544 (1.4, sh)	661 (1.3)
1e	388 (5.1)			
2e	402 (2.8)	481 (3.5)	591 (0.7, sh)	721 (0.6)
3e	385 (7.2)	454 (8.2)	539 (1.6, sh)	678 (1.4)
[Re(bpy)(CO)$_3$Br] [18]	370			
[Re(*mer*-NNN)(CO)$_2$Cl] [44]	367	485	≈ 620	≈ 720
[Re(*fac*-dqp)(CO)$_3$]Cl [42]	340			

Electrochemistry

To further confirm the trend observed by IR and absorption spectroscopy and predicted by the theoretical model, we investigated all complexes by cyclic voltammetry in *N*,*N*-dimethylformamide, using a three electrodes set-up, tetrabutylammonium hexafluorophosphate (TBAP, 0.1 M) as electrolyte and ferrocene as internal reference (0.45 V *vs.* SCE). We used DMF as a solvent due to the limited solubility of the neutral complexes **1a-e** and **2a-e**. The values are reported in Table 3, along with literature values for chloride and triflate analogous complexes.[41, 58] The typical electrochemical profile are illustrated in Figure 6 for the complexes based on the ligand **La**, while the cyclic voltammograms of all complexes are reported in Fig. S35-S51.

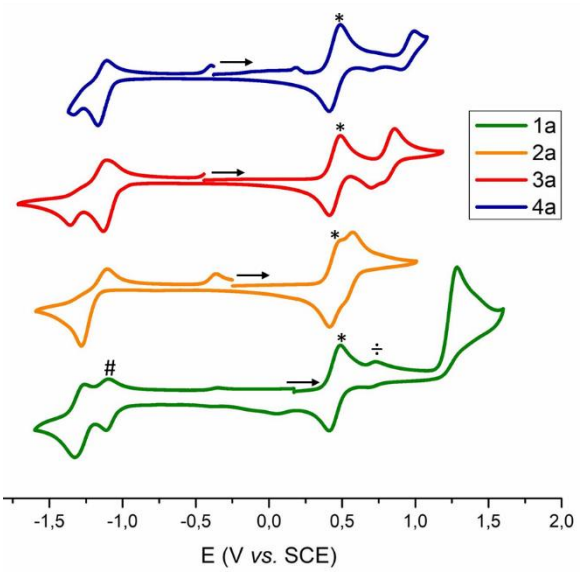

Figure 6 Cyclic voltammograms of all complexes based on ligand La (0.1 mM in DMF, 0.1 M TBAP) with the internal reference Fc^{+}/Fc couple (0.45 V) shown (*). In the case of complex 1a (green), the process attributed to released Br^{-} is shown (÷) while the first reduction event (#) only appear when the oxidation process around 1.4 V as discussed.

Of note is the fact that several of the redox events appear quasi reversible, both chemically and electrochemically (based on the peak separation, ΔE, and the difference between anodic and cathodic currents) and even irreversible in some cases where no return wave observed, as observed for other Re(I) carbonyl complexes.[47, 58, 59] This lack of reversibility can be attributed to an ECE mechanism where a chemical reaction takes place after injection or removal of electron(s), leading to the formation of new species with slightly different redox potentials. Evidences of such mechanism have been reported, see for example the work from Bullock and coworkers on the oxidative disproportionation of Re bipyridine complexes, leading to the formation of a solvent adduct and free bromine.[59] Interestingly, Dempsey and coworkers showed that using very high scan rate, from 500 mV/s up to 100V/s, can restore the reversibility, although only partially in some cases,.[47]

In the cyclic voltammograms of complexes **1a-e** and **2a-e**, we observed the appearance of an additional process of variable intensity around 0.76 V *vs.* SCE (shown on Fig. 6 for **1a**), which corresponds to the reported redox potential of Br_2/Br^{-} in acetonitrile, indicating that a similar decomposition to the one described by Bullock and coworkers is in play.[59, 60] A second complication in the electrochemical measurements came from the tendency of these compounds to adsorb at the surface of the glassy carbon electrode. The working electrode was thus polished between each scan. Finally, in some cases, addition of ferrocene as an internal standard affected the redox events and can be seen in the

comparison between cyclic voltammogram with and without ferrocene presented in the supporting information (see Fig. S35-S51).

Looking first at the reduction potentials, there is little variation between compounds based on the same ligand with different coordination mode, though the cationic complexes **3** and **4** are slightly easier to reduce than the corresponding neutral complexes **1** and **2**. Charge effect aside, this lack of variation is expected based on the ligand-based character of the LUMOs of all complexes, as discussed in the DFT section. There is however a clear correlation between the reduction potentials and the nature of the terpyridine substituents, the complexes based on ligand **Le** with an electron accepting 4-pyridyl substituent being the easiest to reduce (E_{red} around -1 V *vs.* SCE), while the more electron rich ligand **Lb** makes the corresponding complexes harder to reduce (E_{red} around -1.4 V *vs.* SCE). In some complexes, additionnal reduction processes are observed, though they are irreversible in all cases.

In contrast, we were expecting large variation in the oxidation potential between each series of compounds, reflecting on the relative position of the HOMO levels, as observed in the DFT study. The expected trend is indeed observed, with the κ^3N bromide complexes (**2a-e**) being easier to oxidize than the κ^3N pyridine cationic species (**3a-e**), followed by the κ^3N triphenylphosphine form (**4a-b**) and finally the κ^2N complexes (**1a-e**) being the most difficult to oxidize. The oxidation potentials are reduced by 800 mV going from **1a-e** to **2a-e**, matching the predicted destabilization of the HOMO levels centered on the {$Re(CO)_n$} moieties. Interestingly, in addition to the large shift in potential, conversion from κ^2N to κ^3N coordination makes the oxidation processes reversible and reveals that complexes based on the more electron donating 4,4',4''-trimethyl-2,2';6',2''-terpyridine ligand **Lb** are easier to oxidize, by around 100 mV, compare to the other complexes.

Overall, the absorption and electrochemical properties confirmed the predicted trend regarding the change in electronic properties accompanying the variation in 1) coordination mode of the terpyridine ligand, and 2) the nature of the ancillary ligand (Br^-, pyridine or triphenylphosphine). These changes are caused by a destabilization of the highest occupied levels upon conversion from bidentate (κ^2N) to terdentate (κ^3N)

coordination of the terpyridine ligands, as shown by the large variation in oxidation potential, which leads to reduced band gap and lower absorption maxima. Based on this, we decided to look at the emission properties of our complexes, based on the recent report of a near-infrared emission band at room temperature for **3e**,[36] hoping to observe a similar correlation between emission maxima and structure of the compounds.

Table 3 Redox potentials of the different Re(I) complexes (V *vs.* SCE)

	E_{ox} (ΔE / mV)		E_{red} (ΔE / mV)	
1a [a]	1.31 (irr)		-1.30 (77)	
2a [a]	0.55 (52)		-1.31 (qr)	
3a [a]	0.82 (91)		-1.14 (qr)	-1.38 (irr)
4a [a]	0.95 (89)		-1.11 (80)	
1b [a]	1.42 (irr)		-1.40 (155)	
2b [a]	0.45 [d]		-1.42 (qr)	
3b [a]	0.77 (144)		-1.25 (qr)	
4b [a]	0.80 (qr)	1.21 (irr)	-1.38 (qr)	-1.68 (irr)
1c [a]	1.23 (irr)		-1.25 (63)	-1.74 (irr)
2c [a]	0.55 (63)		-1.27 (qr)	
3c [a]	0.82 (63)		-1.11 (qr)	-1.35 (irr)
1d [a]	1.19 (irr)		-1.25 (60)	-1.70 (irr)
2d [a]	0.50 (76)	1.26 (irr)	-1.26 (irr)	
3d [a]	0.81 (69)		-1.11 (qr)	-1.29 (irr)
1e [a]	1.45 (irr)		-0.99 (79)	-1.16 (irr) | -1.33 (irr)
2e [a]	0.56 (48)		-0.89 (95) [d]	-1.23 (irr)
3e [a]	0.83 (77)		-0.96 (qr)	-1.27 (qr)
$[Re(\kappa^2N\text{-tpy})(CO)_3Cl]$ [b]	1.19		-1.34	
$[Re(\kappa^3N\text{-tpy})(CO)_3Cl]$ [c]	0.48 (65)	1.22 (irr)	-1.17 (irr)	-1.34 (irr)
$[Re(\kappa^3N\text{-tpy})(CO)_2(py)](OTf)]$ [c]	0.86 (irr)	1.35 (irr)	-1.21 (irr)	
$[Re(\kappa^3N\text{-tpy})(CO)_2(PPh_3)](OTf)]$ [c]	0.94 (irr)	1.31 (irr)	-1.19 (irr)	

irr. irreversible; qr. quasi reversible (see text); [a] measured in DMF/TBAP 0.1 M; [b] ref. 58, measured in MeCN/TBAP, initially reported *vs.* Fc^+/Fc; [c] ref. 41, measured in MeCN/TBAP; [d] affected by the addition of ferrocene

Luminescence spectroscopy

The emission spectra of the complexes were acquired in acetonitrile (concentrations from 20 to 50 μM). All emissive compounds present broad, non-structured bands and the related photophysical data are reported in Table 4.

The κ^2N complexes **1a-e** emit around 650 nm (Fig. S69). The emission wavelengths vary with the substituent of the terpyridine from 625 nm for the electron rich ligand **Lb** to 682 nm for the electron poor ligand **Le**. The emission maxima and quantum yields are similar to those reported for related chlorine complexes, though the quantum yield of the bromine derivatives prepared here are lower.[19] Noteworthy, **1c** is presenting a double emission band. A similar behaviour was observed for a chlorine substituted counterpart based on **Ld** where the authors attribute the higher energy emission band to a ^{3}LC (π-π* transition).[19] Our TD-DFT analysis indicate that the lowest energy triplet state of **1c** has some ^{3}LC character mixed with contribution from a bromide to ligand charge transfer (Fig. S20). The fact that the bromide contributes to the excited state would explain the variation between bromide and chloride substituted complexes.

Conversion to the neutral κ^3N complexes **2a-e** resulted in a redshift of the lower absorption maxima. These complexes appear, however, to be non-emissive at room temperature, despite the emission predicted by TD-DFT at wavelengths longer than 900 nm. Exchanging the bromide ligand for pyridine or triphenylphosphine caused a blueshift of the lowest absorption maxima and the TD-DFT predicted emission values follow the same trend. These complexes are indeed emissive in the NIR region, with maxima between 780 and 950 nm (Fig. S70-S71).

When looking at the emission maxima of complexes **3a-e**, the same substituent effect than in absorption maxima is observed, with complex **3b** emitting at 840 nm while **3e** emits at 950 nm. The triphenylphosphine complexes **4a-b** emit at higher energies (800 and 782 nm, respectively), in agreement with the stronger blueshift observed in absorption compared to the pyridine complexes **3a-b**. These cationic Re(I) complexes are amongst the most NIR emissive Re(I) complexes.[61] In general, the quantum yields of the cationic complexes **3a-e** and **4a-b** are even higher than those of the neutral κ^2N complexes **1a-e**, a remarkable result for NIR emitting species. As discussed in the theoretical section, it is interesting to recall that among these series there is a change in nature of the emissive state. Indeed, while the κ^2N-tpy halide complexes have a complex mix of MLCT, LLCT and LC contributions in their lowest transition, in the κ^3N complexes, the lowest transition are purely metal-ligand-to-ligand (MLLCT) in nature,

the density being transferred from the {$Re(CO)_2$} fragment to the terpyridine ligand π^* orbital.

Table 4 Emission data for different Re(I) complexes in deaerated acetonitrile at RT.

	1a	**1b**	**1c**	**1d**	**1e**	**2a**	**2b**	**2c**	**2d**	**2e**
λ_{em} / *nm*	640	625	527 653	659	682	N.D.	N.D.	N.D.	N.D.	N.D.
Φ / %[a]	0.03	0.05	0.10	0.05	0.01	-	-	-	-	-
	3a	**3b**	**3c**	**3d**	**3e**	**4a**	**4b**			
λ_{em} / *nm*	870	840	876	865	950	800	782			
Φ / %[b]	0.13	0.18	0.13	0.11	0.02	0.71	0.40			
	[$Re(bpy)(CO)_3Br$][c]			[$Re(bqp\text{-}\kappa^3N)(CO)_3$]$^{+}$ [d]			[$Re(\kappa^3N\text{-pydiimine})(CO)_2X$][e]			
λ_{em} / *nm*	575			606			N.D.			

N.D. not detected; [a] determined relative to [$Re(bpy)(CO)_3Cl$] with Φ = 0.5 %[2]; b determined relative to IR125 with Φ = 23 %[62]; [c] ref. 18; [d] ref. 44, [e] ref. 42

Conclusion

By varying the coordination modes of terpyridines ligands, their substituent and the nature of the axial ligands L of Re(I) carbonyl complexes of general formula [$Re(\kappa^xN\text{-Rtpy})(CO)_yL]^{n+}$, we were able to tune the electronic and photophysical properties of these complexes. Conversion from κ^2N to κ^3N coordination mode of the terpyridine ligands has a major impact on the HOMO levels of these complexes which are destabilized by almost 800 meV, a shift observed in the electrochemical analysis, while the LUMO levels remain unchanged. The HOMO destabilization also leads to a large redshift of the absorption maxima by 300 nm, making the κ^3N bromo complexes **2a-e** panchromatic while the κ^2N bromo complexes **1a-e** were barely absorbing in the visible region. Replacing the bromide ligand by a pyridine (**3a-e**) or a triphenylphosphine ligand (**4a-b**) allows to lessen the HOMO destabilization and is accompanied by blueshifted absorption maxima. These complexes show NIR emission between 780 and 950 nm depending on the ligand used, with unusually high quantum yields between 0.02 and 0.7 % for this class of complexes, attributed to a change in the nature of the excited state. We have thus demonstrated the possibility to finely tune the properties of these complexes via simple structural variations, opening a path to the design of application

specific complexes such as biological probes, a context where NIR emission properties are desirable.[63]

Experimental section

Materials

$Re_2(CO)_{10}$ was obtained from Pressure Chemical and converted to $Re(CO)_5Br$ via titration with bromine.[64] Solvents were of ACS or spectroscopic grade (for absorption and emission measurements) and used as received, like other reagents, from commercial sources (Millipore Sigma or Fisher Scientific). Acetonitrile for electrochemistry was distilled from CaH_2 and stored under N_2. The ligands **La-e** were prepared following published procedures.[65-67] Complexes **1a**, **1e**, **2a**, **2e**, **3a**, **3e** and **4a** were prepared as previously reported and their spectra matched the literature.[36, 41, 50]

Synthetic procedures

The synthetic details and characterization of the Re(I) complexes are provided in the supporting information.

Associated content

Supporting Information

Information regarding instrumentation, synthetic procedures, ^1H NMR spectra, computational (methods, frontier orbitals, natural transition orbitals and optimized coordinates), spectroscopic (absorption, emission) and electrochemical data.

Author information

Corresponding author

*E-mail for G.S.H.: garry.hanan@umontreal.ca

*E-mail for N.Z.: nelsi.zaccheroni@unibo.it

Notes

The authors declare no competing financial interest.

Acknowledgments

G.S.H. thanks the Natural Sciences and Engineering Research Council of Canada for financial support. T.A. thanks the Faculté des Arts et Sciences at Université de Montréal for a Marguerite-Jacques-Lemay scholarship. This research was enabled, in part, by support provided by Compute Canada. N.Z. thanks the Italian Ministry of University and Research (MIUR) for the grant Fondo di Finanziamento Ordinario (FFO).

References

1. Wrighton, M.; Morse, D. L., Nature of the lowest excited state in tricarbonylchloro-1,10-phenanthrolinerhenium(I) and related complexes. *J. Am. Chem. Soc.* **1974,** *96* (4), 998-1003.

2. Caspar, J. V.; Meyer, T. J., Application of the energy gap law to nonradiative, excited-state decay. *J. Phys. Chem.* **1983,** *87* (6), 952-957.

3. Lever, A. B. P., Electrochemical Parametrization of Rhenium Redox Couples. *Inorg. Chem.* **1991,** *30* (9), 1980-1985.

4. Vogler, A.; Kunkely, H., Excited state properties of organometallic compounds of rhenium in high and low oxidation states. *Coord. Chem. Rev.* **2000,** *200*, 991-1008.

5. Kirgan, R. A.; Sullivan, B. P.; Rillema, D. P., Photochemistry and Photophysics of Coordination Compounds: Rhenium. In *Photochemistry and Photophysics of Coordination Compounds II*, Balzani, V.; Campagna, S., Eds. Springer Berlin Heidelberg: Berlin, Heidelberg, 2007; pp 45-100.

6. Veronese, L.; Quartapelle Procopio, E.; Moehl, T.; Panigati, M.; Nonomura, K.; Hagfeldt, A., Triarylamine-based hydrido-carboxylate rhenium(i) complexes as photosensitizers for dye-sensitized solar cells. *Phys. Chem. Chem. Phys.* **2019,** *21* (14), 7534-7543.

7. Kuramochi, Y.; Ishitani, O.; Ishida, H., Reaction mechanisms of catalytic photochemical CO2 reduction using Re(I) and Ru(II) complexes. *Coord. Chem. Rev.* **2018,** *373*, 333-356.

8. Calzaferri, G.; Hädener, K.; Li, J., Photoreduction and electroreduction of carbon dioxide by a novel rhenium(I) p-phenyl-terpyridine carbonyl complex. *J. Photochem. Photobiol., A* **1992,** *64* (2), 259-262.

9. Probst, B.; Kolano, C.; Hamm, P.; Alberto, R., An efficient homogeneous intermolecular rhenium-based photocatalytic system for the production of H_2. *Inorg. Chem.* **2009,** *48* (5), 1836-43.

10. Hawecker, J.; Lehn, J.-M.; Ziessel, R., Efficient photochemical reduction of CO2 to CO by visible light irradiation of systems containing Re(bipy)(CO)3X or Ru(bipy)32+-Co2+ combinations as homogeneous catalysts. *Chem. Comm.* **1983,** (9), 536-538.

11. Sullivan, B. P.; Bolinger, C. M.; Conrad, D.; Vining, W. J.; Meyer, T. J., One- and two-electron pathways in the electrocatalytic reduction of CO2by fac-Re(bpy)(CO)3Cl (bpy = 2,2′-bipyridine). *J. Chem. Soc., Chem. Commun.* **1985,** (20), 1414-1416.

12. Klemens, T.; Switlicka-Olszewska, A.; Machura, B.; Grucela, M.; Schab-Balcerzak, E.; Smolarek, K.; Mackowski, S.; Szlapa, A.; Kula, S.; Krompiec, S.; Lodowski, P.; Chrobok, A., Rhenium(I) terpyridine complexes - synthesis, photophysical properties and application in organic light emitting devices. *Dalton Trans.* **2016,** *45* (4), 1746-62.

13. Wang, D.; Xu, Q. L.; Zhang, S.; Li, H. Y.; Wang, C. C.; Li, T. Y.; Jing, Y. M.; Huang, W.; Zheng, Y. X.; Accorsi, G., Synthesis and photoluminescence properties of rhenium(I) complexes based on 2,2':6',2''-terpyridine derivatives with hole-transporting units. *Dalton Trans.* **2013,** *42* (8), 2716-23.

14. Hostachy, S.; Policar, C.; Delsuc, N., Re(I) carbonyl complexes: Multimodal platforms for inorganic chemical biology. *Coord. Chem. Rev.* **2017,** *351*, 172-188.

15. Wang, F. X.; Liang, J. H.; Zhang, H.; Wang, Z. H.; Wan, Q.; Tan, C. P.; Ji, L. N.; Mao, Z. W., Mitochondria-Accumulating Rhenium(I) Tricarbonyl Complexes Induce Cell Death via Irreversible Oxidative Stress and Glutathione Metabolism Disturbance. *ACS Appl. Mater. Interfaces* **2019,** *11* (14), 13123-13133.

16. Fihri, A.; Artero, V.; Pereira, A.; Fontecave, M., Efficient H_2-producing photocatalytic systems based on cyclometalated iridium- and tricarbonylrhenium-diimine photosensitizers and cobaloxime catalysts. *Dalton Trans.* **2008,** (41), 5567-9.

17. Juris, A.; Campagna, S.; Bidd, I.; Lehn, J. M.; Ziessel, R., Synthesis and photophysical and electrochemical properties of new

halotricarbonyl(polypyridine)rhenium(I) complexes. *Inorg. Chem.* **1988,** *27* (22), 4007-4011.

18. Kurz, P.; Probst, B.; Spingler, B.; Alberto, R., Ligand variations in [ReX(diimine)(CO)(3)] complexes: Effects on photocatalytic CO2 reduction. *Eur. J. Inorg. Chem.* **2006,** *2006* (15), 2966-2974.

19. Klemens, T.; Switlicka-Olszewska, A.; Machura, B.; Grucela, M.; Janeczek, H.; Schab-Balcerzak, E.; Szlapa, A.; Kula, S.; Krompiec, S.; Smolarek, K.; Kowalska, D.; Mackowski, S.; Erfurt, K.; Lodowski, P., Synthesis, photophysical properties and application in organic light emitting devices of rhenium(I) carbonyls incorporating functionalized 2,2 ':6 ',2 "-terpyridines. *RSC Adv.* **2016,** *6* (61), 56335-56352.

20. Klemens, T.; Switlicka, A.; Szlapa-Kula, A.; Krompiec, S.; Lodowski, P.; Chrobok, A.; Godlewska, M.; Kotowicz, S.; Siwy, M.; Bednarczyk, K.; Libera, M.; Mackowski, S.; Pedzinski, T.; Schab-Balcerzak, E.; Machura, B., Experimental and computational exploration of photophysical and electroluminescent properties of modified 2,2 ':6 ',2 "-terpyridine, 2,6-di(thiazol-2-yl)pyridine and 2,6-di(pyrazin-2-yl)pyridine ligands and their Re(I) complexes. *Appl. Organomet. Chem.* **2018,** *32* (12), e4611.

21. Rohacova, J.; Sekine, A.; Kawano, T.; Tamari, S.; Ishitani, O., Trinuclear and Tetranuclear Re(I) Rings Connected with Phenylene, Vinylene, and Ethynylene Chains: Synthesis, Photophysics, and Redox Properties. *Inorg. Chem.* **2015,** *54* (17), 8769-77.

22. Kamecka, A.; Prachnio, K.; Kapturkiewicz, A., The luminescence properties of $[Re(CO)_2(P\text{^}P)(N\text{^}N)]+$ complexes: Comparison with their $[Re(CO)_3(N\text{^}N)(Cl)]$ analogues. *J. Lumin.* **2018,** *203*, 409-419.

23. Loibl, A.; Weber, M.; Lutz, M.; Müller, C., ReI Complexes of Pyridylphosphinines and 2,2′-Bipyridine Derivatives: A Comparison. *Eur. J. Inorg. Chem.* **2019,** *2019* (11-12), 1575-1585.

24. Crawley, M. R.; Kadassery, K. J.; Oldacre, A. N.; Friedman, A. E.; Lacy, D. C.; Cook, T. R., Rhenium(I) Phosphazane Complexes for Electrocatalytic CO2 Reduction. *Organometallics* **2019,** *38* (7), 1664-1676.

25. Addison, C. C.; Davis, R.; Logan, N., Derivatives of pentacarbonylnitratorhenium(I) with some nitrogen, phosphorus, and arsenic donor ligands. *J. Chem. Soc., Dalton Trans.* **1974,** (19), 2070-2071.

26. Tsubaki, H.; Sekine, A.; Ohashi, Y.; Koike, K.; Takeda, H.; Ishitani, O., Control of photochemical, photophysical, electrochemical, and photocatalytic properties of rhenium(I) complexes using intramolecular weak interactions between ligands. *J. Am. Chem. Soc.* **2005,** *127* (44), 15544-55.

27. Morimoto, T.; Nishiura, C.; Tanaka, M.; Rohacova, J.; Nakagawa, Y.; Funada, Y.; Koike, K.; Yamamoto, Y.; Shishido, S.; Kojima, T.; Saeki, T.; Ozeki, T.; Ishitani, O., Ring-shaped Re(I) multinuclear complexes with unique photofunctional properties. *J. Am. Chem. Soc.* **2013,** *135* (36), 13266-9.

28. Mukuta, T.; Simpson, P. V.; Vaughan, J. G.; Skelton, B. W.; Stagni, S.; Massi, M.; Koike, K.; Ishitani, O.; Onda, K., Photochemical Processes in a Rhenium(I) Tricarbonyl N-Heterocyclic Carbene Complex Studied by Time-Resolved Measurements. *Inorg. Chem.* **2017,** *56* (6), 3404-3413.

29. Yam, V. W.-W.; Lau, V. C.-Y.; Cheung, K.-K., Luminescent Rhenium(I) Carbon Wires: Synthesis, Photophysics, and Electrochemistry. X-ray Crystal Structure of [Re(tBu_2bpy)$(CO)_3$(C∶CC∶C)Re(tBu_2bpy)$(CO)_3$]. *Organometallics* **1996,** *15* (6), 1740-1744.

30. Chung, W. K.; Ng, M.; Zhu, N. Y.; Siu, S. K. L.; Yam, V. W. W., Synthesis, characterization and computational studies of luminescent rhenium(I) tricarbonyl diimine complexes with 8-hydroxyquinoline-containing alkynyl ligands. *J. Organomet. Chem.* **2017,** *847*, 278-288.

31. Larsen, C. B.; Wenger, O. S., Photophysics and Photoredox Catalysis of a Homoleptic Rhenium(I) Tris(diisocyanide) Complex. *Inorg. Chem.* **2018,** *57* (6), 2965-2968.

32. Ko, C. C.; Lo, L. T.; Ng, C. O.; Yiu, S. M., Photochemical synthesis of intensely luminescent isocyano rhenium(I) complexes with readily tunable structural features. *Chem. Eur. J.* **2010,** *16* (46), 13773-82.

33. Dinolfo, P. H.; Williams, M. E.; Stern, C. L.; Hupp, J. T., Rhenium-based molecular rectangles as frameworks for ligand-centered mixed valency and optical electron transfer. *J. Am. Chem. Soc.* **2004,** *126* (40), 12989-3001.

34. Laramee-Milette, B.; Lachance-Brais, C.; Hanan, G. S., Synthesis of discrete Re(I) di- and tricarbonyl assemblies using a [4 x 1] directional bonding strategy. *Dalton Trans.* **2015,** *44* (1), 41-5.

35. Rohacova, J.; Ishitani, O., Rhenium(i) trinuclear rings as highly efficient redox photosensitizers for photocatalytic CO_2 reduction. *Chem. Sci.* **2016,** *7* (11), 6728-6739.

36. Laramee-Milette, B.; Zaccheroni, N.; Palomba, F.; Hanan, G. S., Visible and Near-IR Emissions from k(2) N- and k(3) N-Terpyridine Rhenium(I) Assemblies Obtained by an [nx1] Head-to-Tail Bonding Strategy. *Chem. Eur. J.* **2017,** *23* (26), 6370-6379.

37. Wang, C.; Xie, Z.; deKrafft, K. E.; Lin, W., Doping metal-organic frameworks for water oxidation, carbon dioxide reduction, and organic photocatalysis. *J. Am. Chem. Soc.* **2011,** *133* (34), 13445-54.

38. Popov, D. A.; Luna, J. M.; Orchanian, N. M.; Haiges, R.; Downes, C. A.; Marinescu, S. C., A 2,2'-bipyridine-containing covalent organic framework bearing rhenium(i) tricarbonyl moieties for CO2 reduction. *Dalton Trans.* **2018,** *47* (48), 17450-17460.

39. Abel, E. W.; Dimitrov, V. S.; Long, N. J.; Orrell, K. G.; Osborne, A. G.; Pain, H. M.; Šik, V.; Hursthouse, M. B.; Mazid, M. A., 2,2′:6′,2″-Terpyridine (terpy) acting as a fluxional bidentate ligand. Part 2. Rhenium carbonyl halide complexes, fac-$[ReX(CO)_3(terpy)]$(X = Cl, Br or I): NMR studies of their solution dynamics, synthesis of cis-$[ReBr(CO)_2(terpy)]$ and the crystal structure of $[ReBr(CO)_3(terpy)]$. *J. Chem. Soc., Dalton Trans.* **1993,** (4), 597-603.

40. Black, D. R.; Hightower, S. E., Preparation and characterization of rhenium(I) dicarbonyl complexes based on the meridionally-coordinated terpyridine ligand. *Inorg. Chem. Commun.* **2012,** *24*, 16-19.

41. Frenzel, B. A.; Schumaker, J. E.; Black, D. R.; Hightower, S. E., Synthesis, spectroscopic, electrochemical and computational studies of rhenium(I) dicarbonyl

complexes based on meridionally-coordinated 2,2':6',2"-terpyridine. *Dalton Trans.* **2013,** *42* (34), 12440-51.

42. Jurca, T.; Chen, W. C.; Michel, S.; Korobkov, I.; Ong, T. G.; Richeson, D. S., Solid-state thermolysis of a fac-rhenium(I) carbonyl complex with a redox non-innocent pincer ligand. *Chem. Eur. J.* **2013,** *19* (13), 4278-86.

43. Pal, A. K.; Hanan, G. S., Structural, electrochemical and photophysical investigations of Re(I)-complexes of kappa(3)N-tridentate heterocyclic ligands. *Dalton Trans.* **2014,** *43* (31), 11811-4.

44. Losey, D. J.; Frenzel, B. A.; Smith, W. M.; Hightower, S. E.; Hamaker, C. G., Tricarbonyl rhenium complex of 2,6-bis(8 '-quinolinyl)pyridine: Synthesis, spectroscopic characterization, X-ray structure and DFT calculations. *Inorg. Chem. Commun.* **2013,** *30*, 46-48.

45. Bulsink, P.; Al-Ghamdi, A.; Joshi, P.; Korobkov, I.; Woo, T.; Richeson, D., Capturing Re(i) in an neutral N,N,N pincer Scaffold and resulting enhanced absorption of visible light. *Dalton Trans.* **2016,** *45* (21), 8885-96.

46. Lee, P. H.; Ko, C. C.; Zhu, N.; Yam, V. W., Metal coordination-assisted near-infrared photochromic behavior: a large perturbation on absorption wavelength properties of N,N-donor ligands containing diarylethene derivatives by coordination to the rhenium(I) metal center. *J. Am. Chem. Soc.* **2007,** *129* (19), 6058-9.

47. Kurtz, D. A.; Brereton, K. R.; Ruoff, K. P.; Tang, H. M.; Felton, G. A. N.; Miller, A. J. M.; Dempsey, J. L., Bathochromic Shifts in Rhenium Carbonyl Dyes Induced through Destabilization of Occupied Orbitals. *Inorg. Chem.* **2018,** *57* (9), 5389-5399.

48. Koike, K.; Tanabe, J.; Toyama, S.; Tsubaki, H.; Sakamoto, K.; Westwell, J. R.; Johnson, F. P.; Hori, H.; Saitoh, H.; Ishitani, O., New synthetic routes to biscarbonylbipyridinerhenium(I) complexes cis,trans-[Re(X2bpy)(CO)2(PR3)(Y)n+ (X2bpy = 4,4'-X2-2,2'-bipyridine) via photochemical ligand substitution reactions, and their photophysical and electrochemical properties. *Inorg. Chem.* **2000,** *39* (13), 2777-83.

49. Kurtz, D. A.; Dhakal, B.; Donovan, E. S.; Nichol, G. S.; Felton, G. A. N., Non-photochemical synthesis of Re(diimine)$(CO)_2$(L)Cl (L = phosphine or phosphite) compounds. *Inorg. Chem. Commun.* **2015,** *59*, 80-83.

50. Abel, E. W.; Long, N. J.; Orrell, K. G.; Osborne, A. G.; Pain, H. M.; Šik, V., The first examples of 2,2′:6′,2″-terpyridine as a fluxional bidentate ligand. *J. Chem. Soc., Chem. Commun.* **1992,** *0* (4), 303-304.

51. Gelling, A.; Noble, D. R.; Orrell, K. G.; Osborne, A. G.; Šik, V., Synthesis and solution fluxionality of rhenium(I) carbonyl complexes of 2,4,6-tris(pyrazolyl)pyrimidines (L), [ReX(CO)$_3$L](X = Cl, Br or I). Isolation and identification of the dinuclear complex [{ReBr(CO)$_3$}2L]. *J. Chem. Soc., Dalton Trans.* **1996,** (14), 3065-3070.

52. Freyer, A.; DiMeglio, C.; Freyer, A., Synthesis and Characterization of (σ^2-terpyridyl)Re(CO)$_3$Cl with Determination of Chemical Ring Exchange Constant. *J. Chem. Educ.* **2006,** *83* (5), 788.

53. Gelling, A.; Orrell, K. G.; Osborne, A. G.; Sik, V., The energetics and mechanism of fluxionality of 2,2 ': 6 ',2 "-terpyridine derivatives when acting as bidentate ligands in transition-metal complexes. A detailed dynamic NMR study. *J. Chem. Soc., Dalton Trans.* **1998,** (6), 937-945.

54. Martin, R. L., Natural transition orbitals. *J. Chem. Phys.* **2003,** *118* (11), 4775-4777.

55. Vlček, A.; Záliš, S., Modeling of charge-transfer transitions and excited states in d6 transition metal complexes by DFT techniques. *Coord. Chem. Rev.* **2007,** *251* (3-4), 258-287.

56. Zalis, S.; Milne, C. J.; El Nahhas, A.; Blanco-Rodriguez, A. M.; van der Veen, R. M.; Vlcek, A., Jr., Re and Br X-ray absorption near-edge structure study of the ground and excited states of [ReBr(CO)3(bpy)] interpreted by DFT and TD-DFT calculations. *Inorg. Chem.* **2013,** *52* (10), 5775-85.

57. Ladouceur, S.; Swanick, K. N.; Gallagher-Duval, S.; Ding, Z. F.; Zysman-Colman, E., Strongly Blue Luminescent Cationic Iridium(III) Complexes with an Electron-Rich Ancillary Ligand: Evaluation of Their Optoelectronic and Electrochemiluminescence Properties. *Eur. J. Inorg. Chem.* **2013,** *2013* (30), 5329-5343.

58. Amoroso, A. J.; Banu, A.; Coogan, M. P.; Edwards, P. G.; Hossain, G.; Malik, K. M., Functionalisation of terpyridine complexes containing the Re(CO)3(+) moiety. *Dalton Trans.* **2010,** *39* (30), 6993-7003.

59. Bullock, J. P.; Carter, E.; Johnson, R.; Kennedy, A. T.; Key, S. E.; Kraft, B. J.; Saxon, D.; Underwood, P., Reactivity of electrochemically generated rhenium (II) Tricarbonyl alpha-diimine complexes: a reinvestigation of the oxidation of luminescent Re(CO)3(alpha-Diimine)Cl and related compounds. *Inorg. Chem.* **2008,** *47* (17), 7880-7.

60. Allen, G. D.; Buzzeo, M. C.; Villagran, C.; Hardacre, C.; Compton, R. G., A mechanistic study of the electro-oxidation of bromide in acetonitrile and the room temperature ionic liquid, 1-butyl-3-methylimidazolium bis(trifluoromethylsulfonyl)imide at platinum electrodes. *J. Electroanal. Chem.* **2005,** *575* (2), 311-320.

61. Xiang, H.; Cheng, J.; Ma, X.; Zhou, X.; Chruma, J. J., Near-infrared phosphorescence: materials and applications. *Chem. Soc. Rev.* **2013,** *42* (14), 6128-85.

62. Wurth, C.; Grabolle, M.; Pauli, J.; Spieles, M.; Resch-Genger, U., Relative and absolute determination of fluorescence quantum yields of transparent samples. *Nat. Protoc.* **2013,** *8* (8), 1535-50.

63. Lee, L. C.; Leung, K. K.; Lo, K. K., Recent development of luminescent rhenium(i) tricarbonyl polypyridine complexes as cellular imaging reagents, anticancer drugs, and antibacterial agents. *Dalton Trans.* **2017,** *46* (47), 16357-16380.

64. Schmidt, S. P.; Trogler, W. C.; Basolo, F., Pentacarbonylrhenium Halides. *Inorg. Synth.* **1990,** *28*, 160-165.

65. Hanan, G.; Wang, J., A Facile Route to Sterically Hindered and Non-Hindered 4′-Aryl-2,2′:6′,2″-Terpyridines. *Synlett* **2005,** *2005* (08), 1251-1254.

66. Cooke, M. W.; Wang, J.; Theobald, I.; Hanan, G. S., Convenient One-Pot Procedures for the Synthesis of 2,2′:6′,2″-Terpyridine. *Synth. Commun.* **2006,** *36* (12), 1721-1726.

67. Robo, M. T.; Prinsell, M. R.; Weix, D. J., 4,4',4"-trimethyl-2,2':6',2"-terpyridine by oxidative coupling of 4-picoline. *J. Org. Chem.* **2014,** *79* (21), 10624-8.